

# Preparation and some properties of chemically vapour-deposited $\text{Si}_3\text{N}_4$ -TiN composite

TOSHIO HIRAI, SHINSUKE HAYASHI

*The Research Institute for Iron, Steel and Other Metals, Tohoku University, Sendai 980, Japan*

Chemically vapour-deposited (CVD)  $\text{Si}_3\text{N}_4$ -TiN composite (a plate with the maximum thickness of 1.9 mm) has been prepared on a graphite substrate using a mixture of  $\text{SiCl}_4$ ,  $\text{TiCl}_4$ ,  $\text{NH}_3$  and  $\text{H}_2$  gases. The CVD was carried out at deposition temperatures,  $T_{\text{dep}}$ , in the range of 1050 to 1450°C, total gas pressures,  $P_{\text{tot}}$ , from 1.33 to 10.7 kPa and gas flow rates of 136 ( $\text{SiCl}_4$ ), 18 ( $\text{TiCl}_4$ ), 120 ( $\text{NH}_3$ ) and 2720 ( $\text{H}_2$ )  $\text{cm}^3 \text{min}^{-1}$ . The deposits thus obtained appeared black. The Ti content in the composites ranged from 2.1 to 24.8 wt % and was found in the form of TiN. The structure of the  $\text{Si}_3\text{N}_4$  matrices varied from amorphous (initially) to the  $\alpha$ - and  $\beta$ -type, with increasing  $T_{\text{dep}}$ . Most of the  $\alpha$ - and  $\beta$ -type deposits had a preferred orientation (001) parallel to the deposition surface. While the deposition surface of the amorphous deposits showed a pebble structure, the surfaces of the  $\alpha$ - and  $\beta$ -type deposits were composed of various kinds of facets. The heat-treating experiment suggested that  $\beta$ - $\text{Si}_3\text{N}_4$  obtained in the present work was formed directly via a vapour phase, and not from crystallization of amorphous  $\text{Si}_3\text{N}_4$  or from transformation of  $\alpha$ - $\text{Si}_3\text{N}_4$ .

## 1. Introduction

One approach in the course of developing a new material is to combine different components of various substances, i.e. the exploration of composites. Compared to the well-known sintering technique for producing composites, the chemical vapour deposition (CVD) technique can be successfully used to prepare composites having components with low sinterability. Some studies have been conducted on producing composites of a  $\text{Si}_3\text{N}_4$  matrix by CVD for application in electronic and high temperature structural uses. As materials for electronic applications,  $\text{Si}_3\text{N}_4$ -Si, with a non-ohmic d.c. conduction property [1],  $\text{Si}_3\text{N}_4$ -Ge, with a reduced stress in the film [2], and  $\text{Si}_3\text{N}_4$ -AlN, with an enhanced charge storage property [3] have been reported. As high temperature structural materials, CVD of a Sialon has been attempted [4]. For the same application CVD of  $\text{Si}_3\text{N}_4$ -Si-SiC composites was also conducted [5].

A  $\text{Si}_3\text{N}_4$ -C composite having an amorphous  $\text{Si}_3\text{N}_4$  matrix with dispersed carbon was prepared by the present authors via CVD of a  $\text{SiCl}_4$ - $\text{NH}_3$ - $\text{H}_2$ - $\text{C}_3\text{H}_8$  system, and it was found that this composite has a good electrical conductivity [6]. Recently, the present authors obtained a  $\text{Si}_3\text{N}_4$ -TiN composite in a plate form from CVD of a  $\text{SiCl}_4$ - $\text{NH}_3$ - $\text{H}_2$ - $\text{TiCl}_4$  system. A brief description on a part of this work has been previously reported [7].

The present paper describes detailed procedures for the preparation of the plate-like  $\text{Si}_3\text{N}_4$ -TiN composite and the influences of CVD conditions on the various characteristics of the resulting composites, such as, its crystal structure, preferred orientation, surface morphology and Ti content.

## 2. Experimental procedure

### 2.1. Sample preparation

The deposits were prepared by adding  $\text{TiCl}_4$  vapour into a  $\text{SiCl}_4$ - $\text{NH}_3$ - $\text{H}_2$  system which was

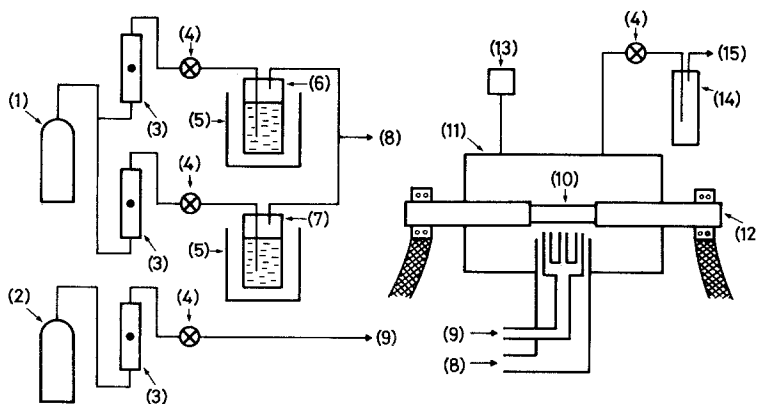


Figure 1 A schematic diagram of the deposition apparatus. (1)  $H_2$  gas, (2)  $NH_3$  gas, (3) flow meter, (4) valve, (5) constant temperature bath, (6)  $SiCl_4$  reservoir, (7)  $TiCl_4$  reservoir, (8)  $SiCl_4 + TiCl_4 + H_2$  gas inlet, (9)  $NH_3$  gas inlet, (10) graphite heater (substrate), (11) reaction chamber, (12) water-cooled electrode, (13) manometer, (14) cold trap and (15) rotary pump.

previously used for the preparation of the CVD- $Si_3N_4$  [8]. The deposition apparatus is schematically illustrated in Fig. 1. The substrate is a graphite plate with dimensions of  $80\text{ mm} \times 25\text{ mm} \times 4\text{ mm}$ . The substrate was heated by applying an electric current. The deposition temperature,  $T_{\text{dep}}$ , was measured using a two-colour pyrometer. The  $SiCl_4$  and  $TiCl_4$  vapours were transported by the  $H_2$  gas by introducing it in the  $SiCl_4$  and  $TiCl_4$  reservoirs which were kept at temperatures of 0 and  $20^\circ\text{C}$ , respectively. The  $H_2$  gas, containing these chloride vapours, was introduced into a reaction chamber through the outer tube of an annular nozzle and  $NH_3$  gas was introduced through the inner tube. The purities of  $SiCl_4$ ,  $TiCl_4$  and  $NH_3$  were 99.9% and that of  $H_2$  was 99.9999%. The total gas pressure,  $P_{\text{tot}}$ , in the reaction chamber was controlled using a needle valve. Table I summarizes the CVD conditions used in the present experiment.

## 2.2. Characterization of samples

The structure of the deposits was examined by an X-ray diffractometer (JEOL DX-GO-S) using Ni-filtered  $CuK\alpha$  radiation. The contents of  $\alpha$ - and  $\beta$ - $Si_3N_4$  in the crystalline deposits were determined from the peak heights of the (201) reflection for the  $\alpha$ -phase, and the (110) reflection for the  $\beta$ -phase, for pulverized samples (under 325 mesh) using a calibration curve for the ratio  $\alpha/\beta$  obtained from the mixtures of  $\alpha$ - and  $\beta$ - $Si_3N_4$

powders. The lattice parameters of  $\alpha$ - and  $\beta$ - $Si_3N_4$  were determined by the Nelson–Riley extrapolation method using the Debye–Scherrer camera. The deposition surface was coated with gold film and observed by a scanning electron microscope (Hitachi Akashi MSM4). The Ti content in the deposits was determined by a chemical analysis.

## 3. Results

Under every CVD condition used in the present experiment the black plate-like deposits were obtained on the graphite substrate. The maximum thickness of the deposit was 1.9 mm.

### 3.1. Crystal structure of the $Si_3N_4$ matrices

Fig. 2 shows the typical X-ray diffraction patterns for pulverized deposit samples. It was found from the X-ray diffraction results that, depending on the CVD condition, the prepared deposits have a matrix consisting of either amorphous,  $\alpha$ - or  $\beta$ - $Si_3N_4$ . In this paper, each of above is denoted as amorphous,  $\alpha$ -type or  $\beta$ -type deposits.

Fig. 3 shows the  $Si_3N_4$  matrix structures found in deposits prepared at various  $T_{\text{dep}}$  and  $P_{\text{tot}}$ . At  $T_{\text{dep}} = 1050$  and  $1150^\circ\text{C}$ , the deposits obtained were amorphous ( $\Delta$ ) irrespective of  $P_{\text{tot}}$  values. At  $T_{\text{dep}} = 1250^\circ\text{C}$  and  $P_{\text{tot}} = 1.33$  to 8 kPa  $\alpha$ -type deposits ( $\bullet$ ) were obtained and at the same  $T_{\text{dep}}$  the amorphous deposit was prepared when  $P_{\text{tot}} = 10.7$  kPa. At  $T_{\text{dep}} = 1350^\circ\text{C}$ , the  $\alpha$ -type deposit was obtained at  $P_{\text{tot}} = 1.33$  kPa,

TABLE I CVD conditions

Deposition temperature, $T_{\text{dep}}$ ( $^\circ\text{C}$ )	Total gas pressure, $P_{\text{tot}}$ (kPa)	Gas flow rate ( $\text{cm}^3\text{ min}^{-1}$ )				Deposition time (h)
		$SiCl_4$	$TiCl_4$	$NH_3$	$H_2$	
1050–1450	1.33–10.7	136	18	120	2720	4–8

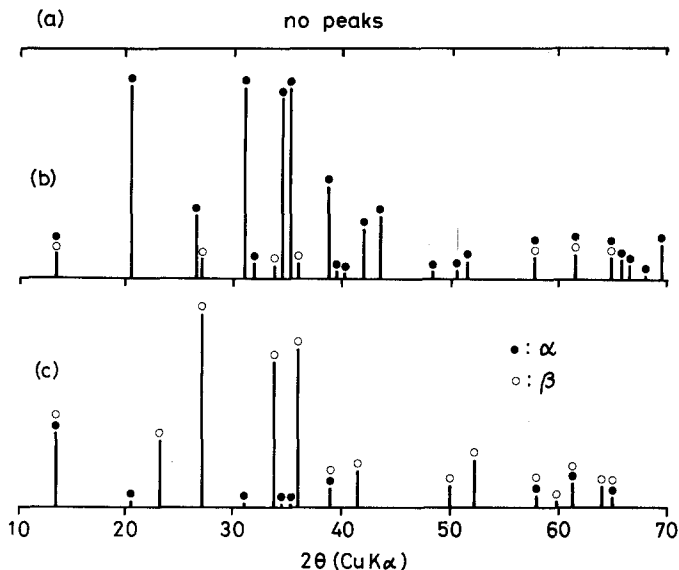


Figure 2 X-ray diffraction patterns of pulverized samples. (a)  $T_{\text{dep}} = 1150^\circ\text{C}$ ,  $P_{\text{tot}} = 4\text{ kPa}$ ; (b)  $T_{\text{dep}} = 1250^\circ\text{C}$ ,  $P_{\text{tot}} = 4\text{ kPa}$ ; (c)  $T_{\text{dep}} = 1350^\circ\text{C}$ ,  $P_{\text{tot}} = 4\text{ kPa}$ .

while the  $\beta$ -type deposits ( $\circ$ ) were obtained at  $P_{\text{tot}} = 4$  to  $10.7\text{ kPa}$ . At  $T_{\text{dep}} = 1450^\circ\text{C}$ , the  $\beta$ -type deposits were prepared at every  $P_{\text{tot}}$ .

Fig. 4 demonstrates the relationship between  $T_{\text{dep}}$  and  $\beta\text{-Si}_3\text{N}_4$  content, i.e.  $\beta/(\alpha + \beta)$ , in the crystalline deposits. At  $P_{\text{tot}} = 1.33\text{ kPa}$ ,  $\beta/(\alpha + \beta)$  is as low as 4 to 9 wt % when  $T_{\text{dep}} = 1250$  and  $1350^\circ\text{C}$ , but it has a value as high as 91 wt % at  $T_{\text{dep}} = 1450^\circ\text{C}$ . At  $P_{\text{tot}} = 4$  to  $10.7\text{ kPa}$ ,  $\beta/(\alpha + \beta)$  was 95 to 100 wt % at  $T_{\text{dep}} = 1350$  and  $1450^\circ\text{C}$ .

The lattice parameters,  $a_o$  and  $c_o$ , of  $\beta\text{-Si}_3\text{N}_4$  obtained at  $T_{\text{dep}} = 1350^\circ\text{C}$  and  $P_{\text{tot}} = 4\text{ kPa}$  and those of  $\alpha\text{-Si}_3\text{N}_4$  obtained at  $T_{\text{dep}} = 1250^\circ\text{C}$  and

$P_{\text{tot}} = 4\text{ kPa}$  were determined. The values of  $a_o$  and  $c_o$  of  $\beta\text{-Si}_3\text{N}_4$  were  $0.7609$  and  $0.2909\text{ nm}$ , respectively. Those of  $\alpha\text{-Si}_3\text{N}_4$  were  $0.7758$  and  $0.5622\text{ nm}$ , respectively.

### 3.2. Preferred orientation

Fig. 5 shows typical X-ray diffraction patterns for deposition surfaces of the crystalline deposits. While the deposit prepared at  $T_{\text{dep}} = 1250^\circ\text{C}$  and  $P_{\text{tot}} = 1.33\text{ kPa}$  gave a strong diffraction peak of  $\alpha(112)$  (Fig. 5a), that prepared at  $T_{\text{dep}} = 1250^\circ\text{C}$  and  $P_{\text{tot}} = 4\text{ kPa}$  gave a strong diffraction peak of  $\alpha(004)$  (Fig. 5b). As for the  $\beta$ -type

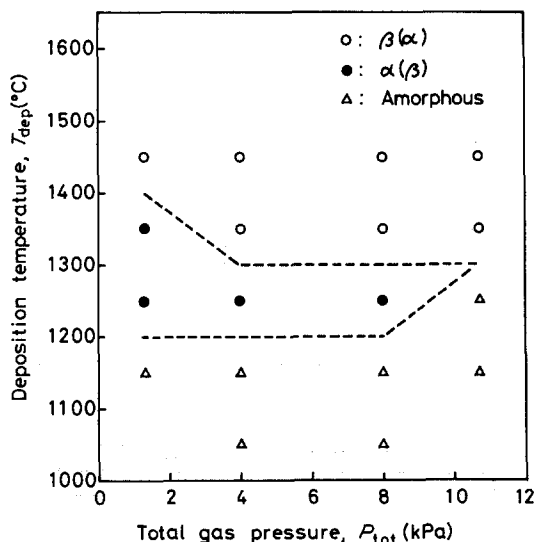


Figure 3 Effect of  $T_{\text{dep}}$  and  $P_{\text{tot}}$  on the structure of  $\text{Si}_3\text{N}_4$  matrices.

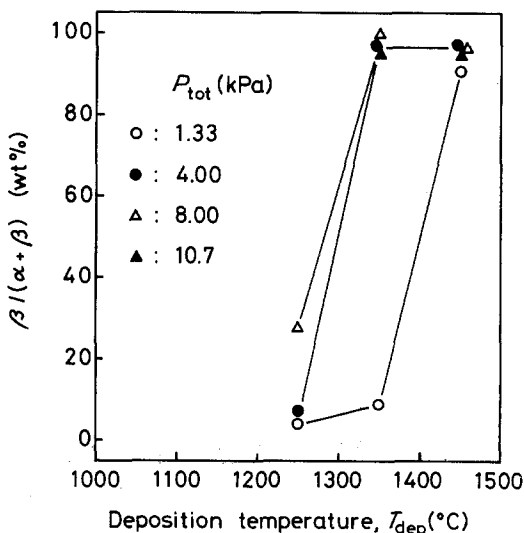


Figure 4 Effect of  $T_{\text{dep}}$  on the content of  $\beta\text{-Si}_3\text{N}_4$ ,  $\beta/(\alpha + \beta)$ , in the crystalline deposits.

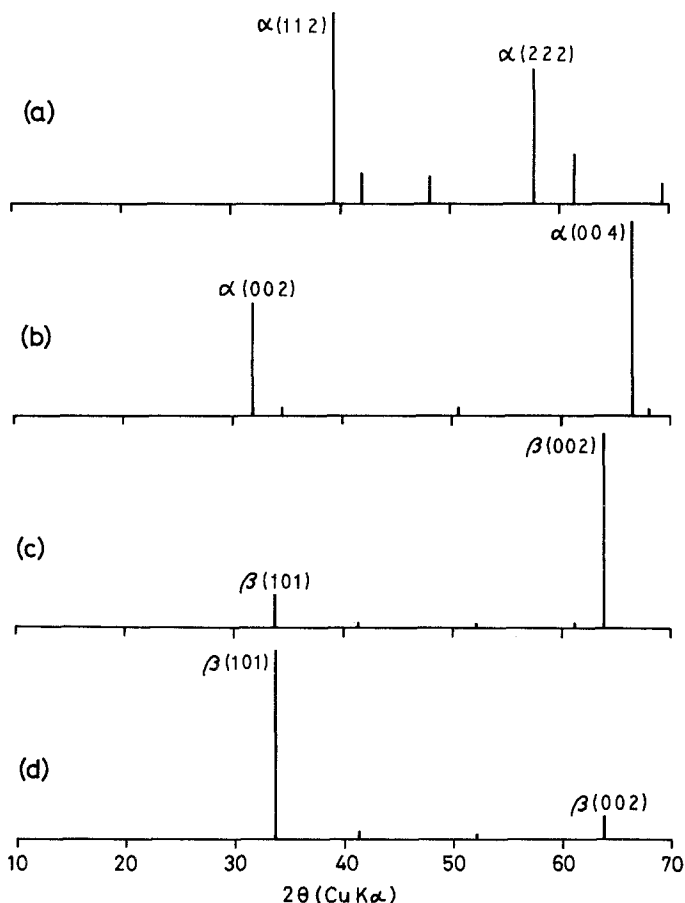


Figure 5 X-ray diffraction patterns for deposition surfaces of the crystalline deposits. (a)  $T_{\text{dep}} = 1250^\circ \text{C}$ ,  $P_{\text{tot}} = 1.33 \text{ kPa}$ ; (b)  $T_{\text{dep}} = 1250^\circ \text{C}$ ,  $P_{\text{tot}} = 4 \text{ kPa}$ ; (c)  $T_{\text{dep}} = 1350^\circ \text{C}$ ,  $P_{\text{tot}} = 4 \text{ kPa}$ ; (d)  $T_{\text{dep}} = 1350^\circ \text{C}$ ,  $P_{\text{tot}} = 10.7 \text{ kPa}$ .

deposits, two types of preferred orientations were observed; a diffraction peak of  $\beta(002)$  was dominant at  $T_{\text{dep}} = 1350^\circ \text{C}$  and  $P_{\text{tot}} = 4 \text{ kPa}$  (Fig. 5c), while  $\beta(101)$  was strong at  $T_{\text{dep}} = 1350^\circ \text{C}$  and  $P_{\text{tot}} = 10.7 \text{ kPa}$  (Fig. 5d).

Table II summarizes the preferred orientation of the crystalline deposits prepared at the various  $T_{\text{dep}}$  and  $P_{\text{tot}}$ . Most of the  $\alpha$ -type deposits showed the (001) preferred orientation. The  $\beta$ -type

deposits showed the (001) preferred orientation at lower  $T_{\text{dep}}$  and  $P_{\text{tot}}$  and the (101) preferred orientation at higher  $T_{\text{dep}}$  and  $P_{\text{tot}}$ .

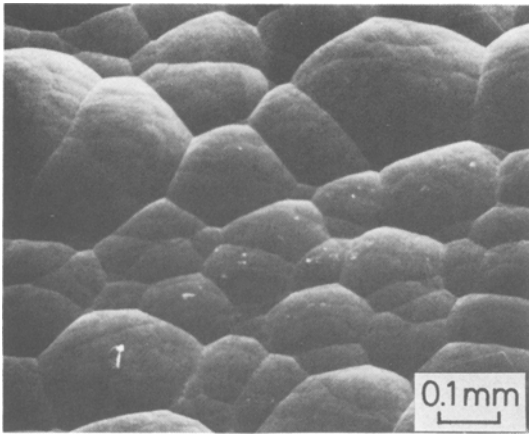
### 3.3. Surface morphology

Fig. 6 shows a typical scanning electron micrograph for the deposition surface of the amorphous deposits. All the amorphous deposits had a pebble structure as shown in Fig. 6. The size of the pebbles ranged from 0.1 to 0.4 mm and remained practically constant with  $T_{\text{dep}}$  and  $P_{\text{tot}}$ .

The surface morphology of the crystalline deposits was markedly different from that of the amorphous deposits. Fig. 7 shows that scanning electron micrographs for the deposition surfaces of the  $\alpha$ -type deposits obtained at  $T_{\text{dep}} = 1250^\circ \text{C}$  and  $P_{\text{tot}} = 1.33$  to 8 kPa. The deposit prepared at  $P_{\text{tot}} = 1.33 \text{ kPa}$  had a pebble-like structure as shown in Fig. 7a, however, the observation at a higher magnification revealed that those pebbles were actually composed of crystalline facets (Fig. 7b). This deposit has a (112) preferred orientation. At  $P_{\text{tot}} = 4 \text{ kPa}$ , the deposits were

TABLE II Preferred orientation of the crystalline deposits

$T_{\text{dep}} (^\circ \text{C})$	$P_{\text{tot}} (\text{kPa})$	Strongest diffraction peak
1250	1.33	$\alpha(112)$
1250	4	$\alpha(004)$
1250	8	$\alpha(004)$
1350	1.33	$\alpha(004)$
1350	4	$\beta(002)$
1350	8	$\beta(002)$
1350	10.7	$\beta(101)$
1450	1.33	$\beta(002)$
1450	4	$\beta(002)$
1450	8	$\beta(101)$
1450	10.7	$\beta(101)$



**Figure 6** A scanning electron micrograph of the amorphous deposit prepared at  $T_{\text{dep}} = 1050^\circ \text{C}$  and  $P_{\text{tot}} = 4 \text{ kPa}$ .

in the form of hexagonal pyramids with sizes of 0.1 to 0.3 mm having a preferred orientation of (001) (Fig. 7c). At  $P_{\text{tot}} = 8 \text{ kPa}$ , they appeared as grains of sizes 0.1 to 0.2 mm, consisting of piled up hexagonal plates with a preferred orientation of (001) (Fig. 7d).

Fig. 8 shows the scanning electron micrographs for the deposition surfaces of the  $\beta$ -type deposits prepared at  $T_{\text{dep}} = 1450^\circ \text{C}$  and  $P_{\text{tot}} = 1.33$  to 10.7 kPa. At  $P_{\text{tot}} = 1.33 \text{ kPa}$ , they appeared as grains with sizes below 0.1 mm. Their facets were observed to be not well developed (Fig. 8a). This deposit had a (001) preferred orientation. At  $P_{\text{tot}} = 8 \text{ kPa}$ , grains consisting of piled  $c$ -facets of  $\beta\text{-Si}_3\text{N}_4$ , having a (001) preferred orientation, were observed (Fig. 8b). At  $P_{\text{tot}} = 10.7 \text{ kPa}$ , the well developed hexagonal  $c$ -facets have appeared

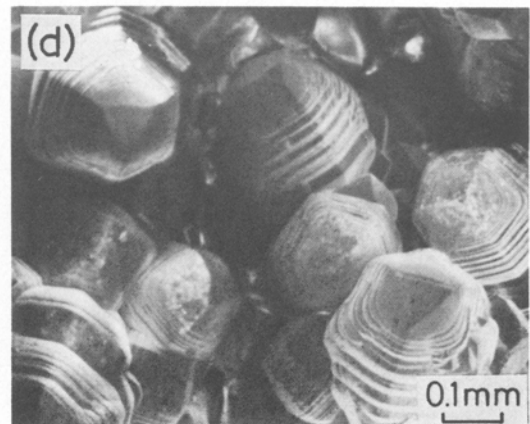
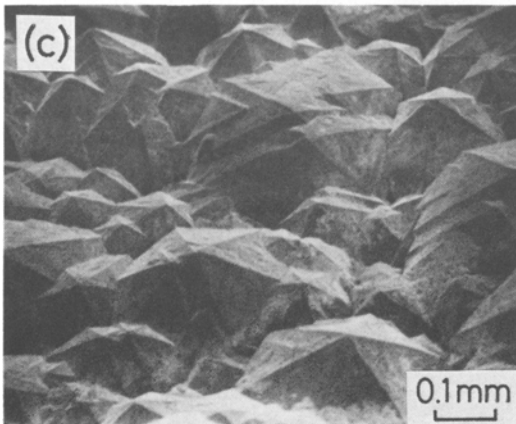
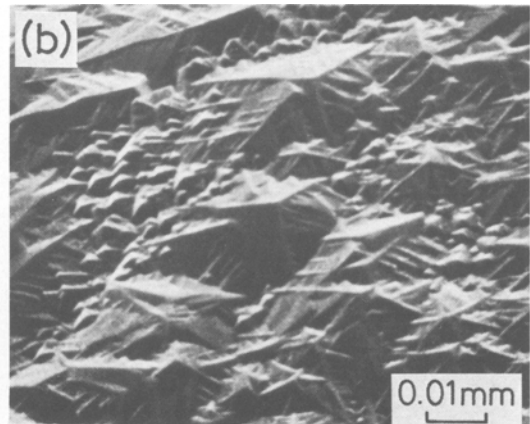
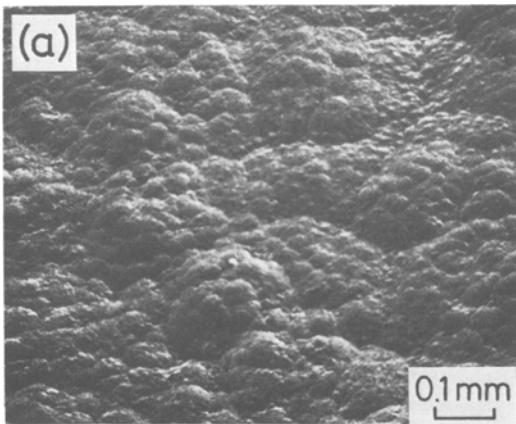


**Figure 7** Scanning electron micrographs of the  $\alpha$ -type deposits prepared at  $T_{\text{dep}} = 1250^\circ \text{C}$ . (a)  $P_{\text{tot}} = 1.33 \text{ kPa}$ ; (b) a higher magnification of (a); (c)  $P_{\text{tot}} = 4 \text{ kPa}$ ; (d)  $P_{\text{tot}} = 8 \text{ kPa}$ .

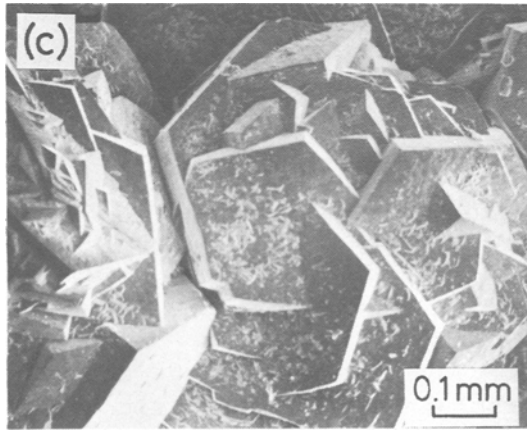
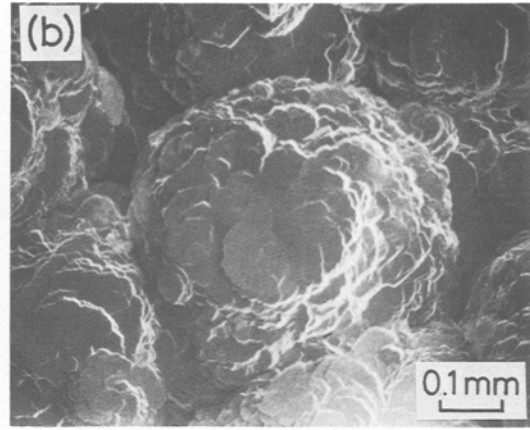
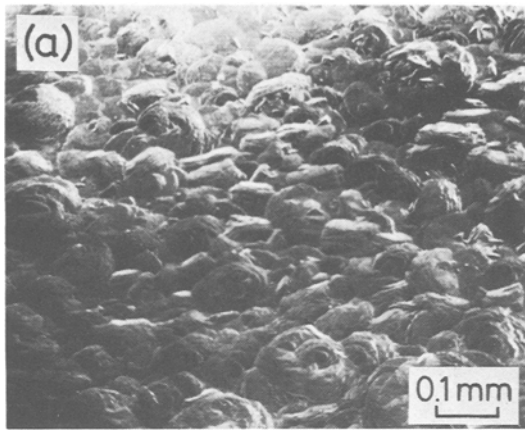


Figure 8 Scanning electron micrographs of the  $\beta$ -type deposits prepared at  $T_{\text{dep}} = 1450^\circ \text{C}$ . (a)  $P_{\text{tot}} = 1.33$  kPa; (b)  $P_{\text{tot}} = 8$  kPa; (c)  $P_{\text{tot}} = 10.7$  kPa.

(Fig. 8c). This deposit had a (101) preferred orientation.

### 3.4. Ti content

Figs 9 and 10 show the influences of  $T_{\text{dep}}$  and  $P_{\text{tot}}$  on the Ti content in the deposits. As is clear from Fig. 9 the Ti content decreases with increasing  $T_{\text{dep}}$  in the  $T_{\text{dep}}$  range of 1050 to 1450°C. In Fig. 10, the Ti content decreases with increasing  $P_{\text{tot}}$  in the range of 1.33 to 4 kPa. The Ti content remained almost constant in the range of 4 to 10.7 kPa at  $T_{\text{dep}}$  between 1150 and 1450°C. The maximum content was 24.8 wt % at  $T_{\text{dep}} = 1150^\circ \text{C}$  and  $P_{\text{tot}} = 1.33$  kPa, and the minimum was 2.1 wt % at  $T_{\text{dep}} = 1450^\circ \text{C}$  and  $P_{\text{tot}} = 8$  kPa.

### 3.5. State of Ti in deposits

Fig. 11 shows an X-ray diffraction pattern of the amorphous deposit having a high Ti content (24.1 wt %) prepared at  $T_{\text{dep}} = 1050^\circ \text{C}$  and  $P_{\text{tot}} = 4$  kPa. Very broad peaks at  $2\theta = 36.6$ ,  $42.5$ , and  $62.0^\circ$  are observed. These peaks correspond to (111), (200) and (220) reflections of

TiN, respectively. From the half-value width of these peaks, the crystallite size of TiN was roughly estimated to be 3 nm. X-ray diffraction peaks of TiN were not detected for the  $\alpha$ - and  $\beta$ -type deposits. This absence of the peaks may be due to the low Ti content and overlapping of the diffraction peaks of TiN with those of  $\alpha$ - and  $\beta$ - $\text{Si}_3\text{N}_4$ . As reported in [9], the existence of TiN in that crystalline deposits was confirmed by a transmission electron microscopic observation. Therefore, the deposits prepared by CVD of the  $\text{SiCl}_4$ - $\text{TiCl}_4$ - $\text{NH}_3$ - $\text{H}_2$  system are composites of  $\text{Si}_3\text{N}_4$ -TiN.

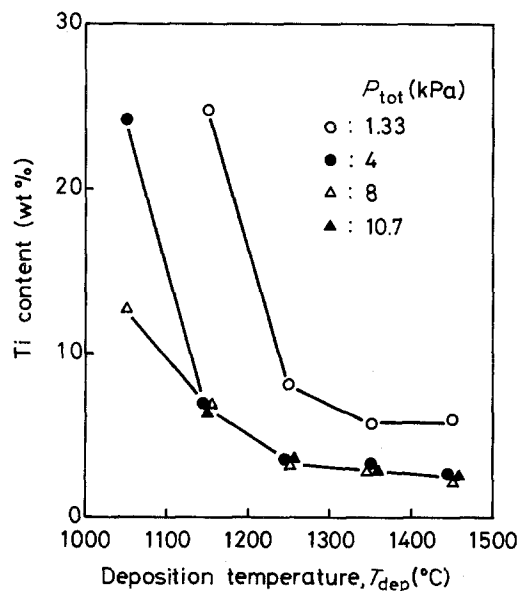


Figure 9 Effect of  $T_{\text{dep}}$  on the Ti content in the deposits.

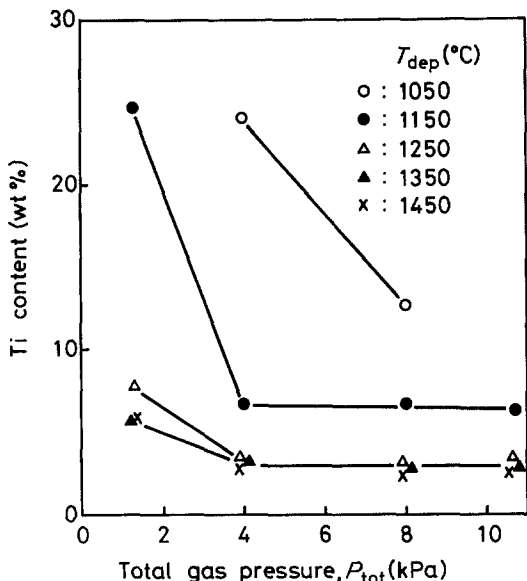


Figure 10 Effect of  $P_{tot}$  on the Ti content in the deposits.

#### 4. Discussion

The structure of CVD- $\text{Si}_3\text{N}_4$  prepared by many investigators in powder, thin film, coating and bulk forms were mostly amorphous or  $\alpha$ -crystalline. In some works [4, 5, 10], however, the formation of  $\beta$ - $\text{Si}_3\text{N}_4$  has been recognized. Landingham and Taylor [4] reported the formation of crystalline deposits composed of  $\alpha$ - $\text{Si}_3\text{N}_4$ ,  $\beta$ - $\text{Si}_3\text{N}_4$ , AlN and some unknown phases at the end of the gas-inlet tube when they performed CVD of a  $\text{SiCl}_4$ - $\text{AlCl}_3$ - $\text{NH}_3$ - $\text{H}_2$ - $\text{O}_2$  for the purpose of preparing a Sialon. However, no description of the  $\beta$ - $\text{Si}_3\text{N}_4$  content was given in their paper. Nickl and Braunmühl [5] obtained a deposit consisting of free Si and  $\alpha$ - $\text{Si}_3\text{N}_4$  at a temperature of  $1300^\circ\text{C}$  from CVD of a  $\text{SiCl}_4$ - $\text{N}_2$ - $\text{H}_2$  mixture, and also reported the observation of some diffraction lines which may be attributed to the existence of  $\beta$ - $\text{Si}_3\text{N}_4$ . Kijima *et al.* [10] obtained a mixture of  $\alpha$ - and  $\beta$ - $\text{Si}_3\text{N}_4$  at 1300 to  $1400^\circ\text{C}$  from CVD of  $\text{SiCl}_4$ - $\text{N}_2$ - $\text{H}_2$  and reported that a large number of crystals were identified as  $\alpha$ - $\text{Si}_3\text{N}_4$ .

For a comparison, CVD of a  $\text{SiCl}_4$ - $\text{NH}_3$ - $\text{H}_2$

system was conducted at the following conditions:  $T_{dep} = 1050$  to  $1450^\circ\text{C}$ ,  $P_{tot} = 4$  kPa and flow rates of 136 ( $\text{SiCl}_4$ ), 120 ( $\text{NH}_3$ ) and 2720 ( $\text{H}_2$ )  $\text{cm}^3 \text{min}^{-1}$ .  $\alpha$ - $\text{Si}_3\text{N}_4$  was formed at  $T_{dep} = 1450^\circ\text{C}$  and amorphous  $\text{Si}_3\text{N}_4$  was obtained at  $T_{dep}$  below  $1350^\circ\text{C}$ . On the other hand, for the  $\text{SiCl}_4$ - $\text{TiCl}_4$ - $\text{NH}_3$ - $\text{H}_2$  system, as shown in Fig. 3,  $\alpha$ - $\text{Si}_3\text{N}_4$  was formed together with a small amount of  $\beta$ - $\text{Si}_3\text{N}_4$  at  $T_{dep} = 1250^\circ\text{C}$ . Moreover,  $\beta$ - $\text{Si}_3\text{N}_4$  was the main product at the higher temperatures of  $T_{dep} = 1350$  and  $1450^\circ\text{C}$ . This result indicates that the addition of  $\text{TiCl}_4$  lowers the deposition temperature of  $\alpha$ - $\text{Si}_3\text{N}_4$  and promotes the formation of  $\beta$ - $\text{Si}_3\text{N}_4$ .

In order to confirm this finding on the effect of adding  $\text{TiCl}_4$ , CVD of the  $\text{SiCl}_4$ - $\text{NH}_3$ - $\text{H}_2$  system was conducted at  $T_{dep} = 1350^\circ\text{C}$  and  $P_{tot} = 4$  kPa, followed by CVD of the  $\text{SiCl}_4$ - $\text{TiCl}_4$ - $\text{NH}_3$ - $\text{H}_2$  system at the same  $T_{dep}$  and  $P_{tot}$ . Fig. 12 shows a scanning electron micrograph of a cross-section of the deposit: Part a corresponds to the amorphous  $\text{Si}_3\text{N}_4$  deposit and Part b is the  $\beta$ -type deposit. In Fig. 12, Parts a and b have different fractographs, corresponding to the characteristics of the amorphous and the polycrystalline ceramics, respectively.

In order to obtain some information on the formation mechanism of  $\beta$ - $\text{Si}_3\text{N}_4$ , a heat-treatment was performed on the amorphous deposit prepared at  $T_{dep} = 1150^\circ\text{C}$  and  $P_{tot} = 4$  kPa from the  $\text{SiCl}_4$ - $\text{TiCl}_4$ - $\text{NH}_3$ - $\text{H}_2$  system. A six hour heat-treatment at a temperature of  $1400^\circ\text{C}$  in Ar flow crystallized amorphous  $\text{Si}_3\text{N}_4$  to  $\alpha$ - $\text{Si}_3\text{N}_4$  but not to  $\beta$ - $\text{Si}_3\text{N}_4$ . On the other hand, as described earlier,  $\beta$ - $\text{Si}_3\text{N}_4$  was obtained at the low  $T_{dep}$  of  $1250^\circ\text{C}$ . These results imply that the formation of  $\beta$ - $\text{Si}_3\text{N}_4$  is a direct result of the CVD process.

The lattice parameters of  $\alpha$ - and  $\beta$ - $\text{Si}_3\text{N}_4$  have been measured by many investigators. The values that have been reported are:  $a_o = 0.7748$  to  $0.7818$  nm and  $c_o = 0.5591$  to  $0.5627$  nm for  $\alpha$ - $\text{Si}_3\text{N}_4$  [11-21] and  $a_o = 0.7595$  to  $0.7609$  nm and  $c_o = 0.2902$  to  $0.2911$  nm for  $\beta$ - $\text{Si}_3\text{N}_4$  [11-15, 22-24]. Because the lattice parameters of  $\alpha$ -

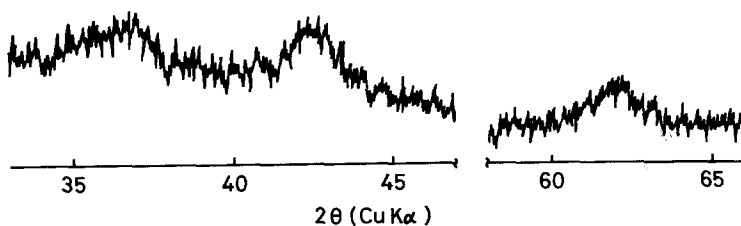


Figure 11 An X-ray diffraction pattern of the amorphous deposit prepared at  $T_{dep} = 1050^\circ\text{C}$  and  $P_{tot} = 4$  kPa.

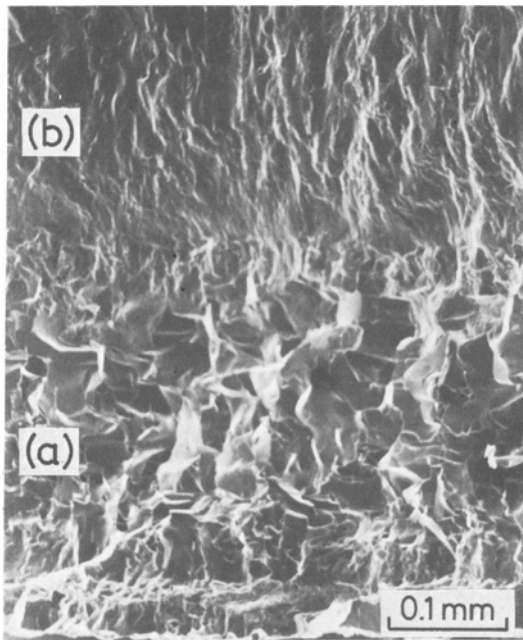


Figure 12 Cross-sectional structure of the deposit prepared at  $T_{\text{dep}} = 1350^{\circ}\text{C}$  and  $P_{\text{tot}} = 4\text{ kPa}$  (a) the amorphous deposit obtained from the  $\text{SiCl}_4\text{-NH}_3\text{-H}_2$  system; (b) the  $\beta$ -type deposit obtained from the  $\text{SiCl}_4\text{-TiCl}_4\text{-NH}_3\text{-H}_2$  system.

and  $\beta\text{-Si}_3\text{N}_4$  matrices found in CVD  $\text{Si}_3\text{N}_4\text{-TiN}$  composites lie in the range of these reported values, the solid solubility of TiN in  $\text{Si}_3\text{N}_4$  is not thought to be significant. At the present time measurement of the lattice parameters for  $\alpha$ - and  $\beta\text{-Si}_3\text{N}_4$ , obtained under different conditions, are underway.

There have been several studies made on the preferred orientation of CVD  $\text{Si}_3\text{N}_4$  ( $\alpha\text{-Si}_3\text{N}_4$ ). Niihara and Hirai [20] reported that the preferred orientation of the  $\alpha\text{-Si}_3\text{N}_4$  deposit from  $\text{SiCl}_4\text{-NH}_3$  was (111) at a low  $P_{\text{tot}}$  and high  $T_{\text{dep}}$  and was (110) and (210) at a high  $P_{\text{tot}}$  and low  $T_{\text{dep}}$ . Moreover, Hirai *et al.* [21] pointed out that in the CVD of the same system the (111) orientation became more prominent as the flow rate of  $\text{SiCl}_4$  is increased. Gebhardt *et al.* [25] found a (001) orientation for an  $\alpha\text{-Si}_3\text{N}_4$  deposit prepared from  $\text{SiCl}_4\text{-NH}_3$ , and a (110) orientation for a deposit from  $\text{SiF}_4\text{-NH}_3$ . Galasso *et al.* [19] conducted a CVD of  $\text{SiF}_4\text{-NH}_3$  and reported that most of the  $\alpha\text{-Si}_3\text{N}_4$  deposits had the (111) orientation but (001) orientation was also sometimes observed. The  $\alpha$ -type deposits obtained in the present study

have none of the (111), (110), and (210) orientations. Although various factors such as the raw materials, the substrate, deposition temperature, gas flow rate, and the total gas pressure have an effect on the preferred orientation, the emergence of the (001) orientation of the  $\alpha$ - and  $\beta$ -type deposits in the present study may be related to the co-deposition of TiN. A configuration of TiN in the  $\text{Si}_3\text{N}_4\text{-TiN}$  composites has been described in [9], forthcoming paper [9].

## 5. Conclusions

(a) CVD of the  $\text{SiCl}_4\text{-TiCl}_4\text{-NH}_3\text{-H}_2$  system was carried out in the range of  $T_{\text{dep}} = 1050$  to  $1450^{\circ}\text{C}$  and  $P_{\text{tot}} = 1.33$  to  $10.7\text{ kPa}$ . In the process a black deposit in the form of plate, with the maximum thickness of  $1.9\text{ mm}$ , was obtained.

(b) The Ti content in the deposits decreased with increasing  $T_{\text{dep}}$  and  $P_{\text{tot}}$ . The maximum content was  $24.8\text{ wt \%}$  at  $T_{\text{dep}} = 1150^{\circ}\text{C}$  and  $P_{\text{tot}} = 1.33\text{ kPa}$ , and the minimum was  $2.1\text{ wt \%}$  at  $T_{\text{dep}} = 1450^{\circ}\text{C}$  and  $P_{\text{tot}} = 8\text{ kPa}$ . Since Ti existed in a form of TiN, the deposits obtained in this study can be explained as composites of  $\text{Si}_3\text{N}_4$  and TiN.

(c) The structure of the  $\text{Si}_3\text{N}_4$  matrices depended on  $T_{\text{dep}}$  and  $P_{\text{tot}}$ . At  $T_{\text{dep}} = 1050$  and  $1150^{\circ}\text{C}$ , the amorphous deposit was obtained. At  $T_{\text{dep}} = 1250^{\circ}\text{C}$ , the crystalline  $\text{Si}_3\text{N}_4$  deposit, mainly consisting of  $\alpha$ -phase ( $72$  to  $96\text{ wt \%}$ ), was formed at  $P_{\text{tot}} = 1.33$  to  $8\text{ kPa}$  and the amorphous deposit was formed at  $P_{\text{tot}} = 10.7\text{ kPa}$ . At  $T_{\text{dep}} = 1350$  and  $1450^{\circ}\text{C}$ , the crystalline deposit, consisting mainly of  $\beta$ -phase ( $91$  to  $100\text{ wt \%}$ ) was preferentially obtained.

(d) The addition of  $\text{TiCl}_4$  to the  $\text{SiCl}_4\text{-NH}_3\text{-H}_2$  system had the effect of lowering the deposition temperature of the  $\alpha\text{-Si}_3\text{N}_4$  and promoting the formation of the  $\beta\text{-Si}_3\text{N}_4$ .

(e) The lattice parameters of  $\alpha$ - and  $\beta\text{-Si}_3\text{N}_4$  in the CVD  $\text{Si}_3\text{N}_4\text{-TiN}$  composites were close to those of pure  $\text{Si}_3\text{N}_4$ . The  $\alpha\text{-Si}_3\text{N}_4$  matrix mainly showed (001) preferred orientation and the  $\beta\text{-Si}_3\text{N}_4$  matrix had (001) and (101) preferred orientations, depending on  $T_{\text{dep}}$  and  $P_{\text{tot}}$ .

(f) The surface morphology of  $\text{Si}_3\text{N}_4\text{-TiN}$  composites well reflected the structure of the  $\text{Si}_3\text{N}_4$  matrix; i.e., while the deposition surface of the amorphous deposits showed the pebble structure, that of the crystalline deposits consisted of various kinds of facets.



## Acknowledgements

The authors wish to express their appreciation to Mr A. Ohkubo for his assistance in preparing the test samples and Mr H. Kimura for carrying out the chemical analysis.

## References

1. D. DONG, E. A. IRENE and D. R. YOUNG, *J. Electrochem. Soc.* **125** (1978) 819.
2. Y. TAMAKI, S. ISOMAE, A. SHINTANI and M. MAKI, *ibid.* **126** (1979) 2271.
3. S. ZIRINSKY and E. A. IRENE, *ibid.* **125** (1978) 305.
4. R. L. LANDINGHAM and R. W. TAYLOR, "Energy and Ceramics", edited by P. Vincenzini (Elsevier New York, 1980) p. 494.
5. J. J. NICKL and C. V. BRAUNMÜHL, *J. Less-Comm. Met.* **37** (1974) 317.
6. T. HIRAI and T. GOTO, *J. Mater. Sci.* **16** (1981) 17.
7. T. HIRAI and S. HAYASHI, *J. Amer. Ceram. Soc.* **64** (1981) C-88.
8. K. NIIHARA and T. HIRAI, *J. Mater. Sci.* **11** (1976) 593.
9. T. HIRAI and S. HAYASHI, Proceedings of the 8th International Conference on CVD, edited by J. M. Blocher, Jr, G. E. Vuillard and G. Wahl (Electrochemical Society, 1981) p. 790.
10. K. KIJIMA, N. SETAKA and H. TANAKA, *J. Crystal Growth* **24/25** (1974) 183.
11. D. HARDIE and K. H. JACK, *Nature* **180** (1957) 332.
12. W. D. FORGENG and B. F. DECKER, *Trans. Metall. Soc. AIME* **212** (1958) 343.
13. S. N. RUDDLESSEN and P. POPPER, *Acta Cryst.* **11** (1958) 465.
14. D. S. THOMPSON and P. L. PRATT, "Science of Ceramics", Vol. 3, edited by G. H. Stewart (Academic Press, New York, 1967) p. 33.
15. S. WILD, P. GRIEVESON and K. H. JACK, "Special Ceramics 5", edited by P. Popper (British Ceramic Research Association, Stoke-on-Trent, 1972) p. 385.
16. R. MARCHAND, Y. LAURENT, J. LANG and M. Th. LEBIHAN, *Acta Cryst.* **B25** (1969) 2157.
17. K. KATO, Z. INOUE, K. KIJIMA, I. KAWADA, H. TANAKA and T. YAMANE, *J. Amer. Ceram. Soc.* **58** (1975) 90.
18. H. F. PRIEST, F. C. BURNS, G. L. PRIEST and E. C. SKAAR, *ibid.* **56** (1973) 395.
19. F. GALASSO, U. KUNTZ and W. J. CROFT, *ibid.* **55** (1972) 431.
20. K. NIIHARA and T. HIRAI, *J. Mater. Sci.* **12** (1977) 1233.
21. T. HIRAI, K. NIIHARA and T. GOTO, *J. Japan Inst. Met.* **41** (1977) 358.
22. L. J. GAUCKLER, H. L. LUKAS and T. Y. TIEN, *Mater. Res. Bull.* **11** (1976) 503.
23. I. C. HUSEBY, H. L. LUKAS and G. PETZOW, *J. Amer. Ceram. Soc.* **58** (1975) 377.
24. R. GRÜN, *Acta Cryst.* **B35** (1979) 800.
25. J. J. GEBHARDT, R. A. TANZILLI and T. A. HARRIS, *J. Electrochem. Soc.* **123** (1976) 1578.

Received 28 August  
and accepted 29 September 1981